2. Light

2.1. Planck radiation law
2.2. Harmonic oscillator and Coherent states
2.3. quantization of electro magnetic field
2.4. The Laser (a reminder)

Radiation Field

modes and quantisation

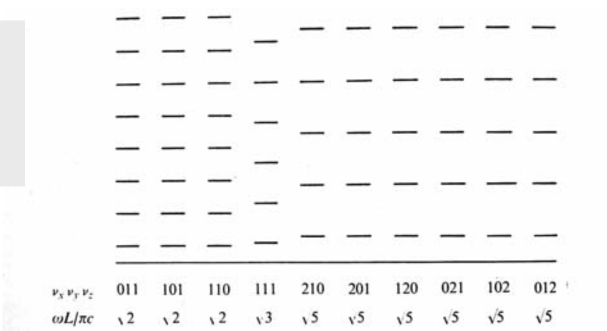

FIG. 1.4. Harmonic oscillator levels for the modes that correspond to the ten points closest to the origin in Fig. 1.2.

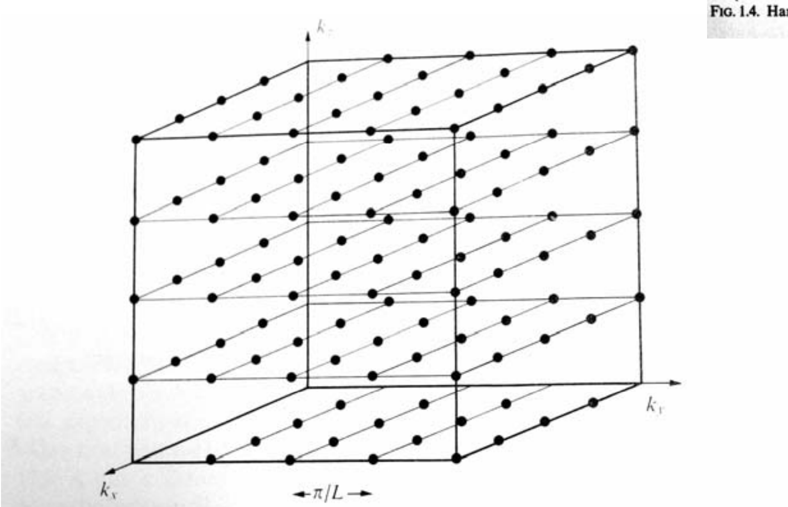

FIG. 1.2. The allowed wavevectors **k** for a cubic cavity of edge L. Note the absence of points for which two or three of the components would be zero.

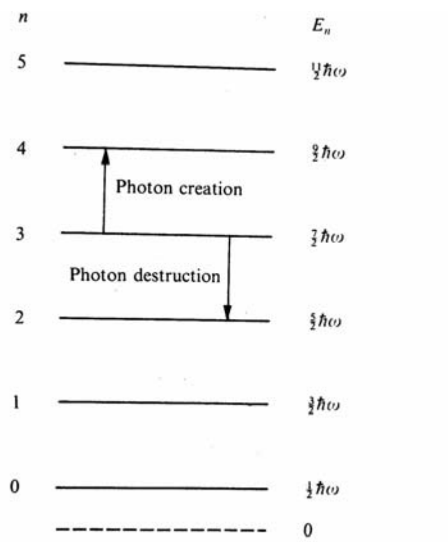

FIG. 1.3. The six lowest energy levels of a quantum harmonic oscillator.

Schwarzkörper-Strahlung
Planck'sches Strahlungsgesetz

Thermisches Gleichgewicht
Wahrscheinlichkeit n-Photonen in einer Mode zu finden

$$P_n = \frac{\exp(-E_n / k_B T)}{\sum_n \exp(-E_n / k_B T)}$$

mit $U = \exp(-\hbar\omega / k_B T)$

$$P_n = \frac{U^n}{\sum_n U^n} \quad \text{mit} \sum_{n=0}^{\infty} U^n = \frac{1}{1-U}$$

$$P_n = (1-U)U^n$$

Mittlere Anzahl von Photonen in einer Mode

$$\bar{n} = \sum_n n P_n = (1-U)\sum_n n U^n = \frac{U}{1-U}$$

$$\bar{n} = \frac{1}{\exp(\hbar\omega / k_B T) - 1}$$

Mittlere Energiedichte Planck'sches Strahlungsgesetz

$$\overline{W}(\omega) d(\omega) = \bar{n}\hbar\omega\, \rho_\omega d(\omega)$$

$$\overline{W}(\omega) d(\omega) = \frac{\hbar\omega^3}{\pi^2 c^3} \frac{d(\omega)}{\exp(\hbar\omega / k_B T) - 1}$$

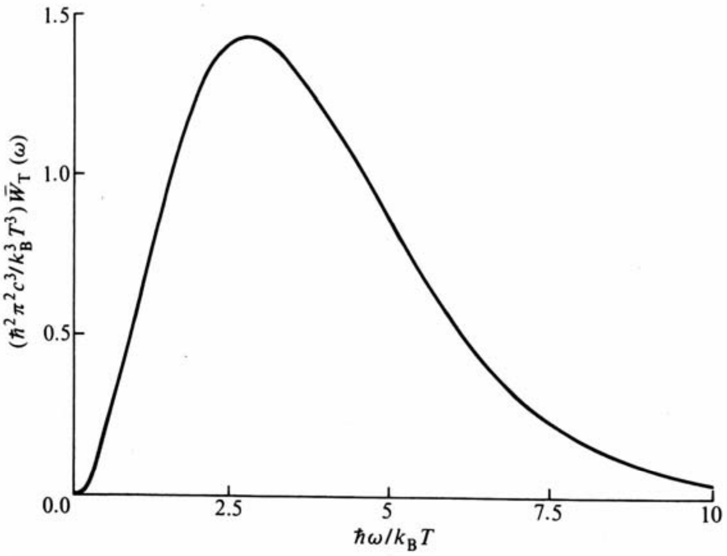

Planck's law for the energy density of electromagnetic radiation at frequency ω and temperature T.

Wien'sches Gesetz $\quad \hbar\omega_{\max} = 2.8\, k_B T$

Stefan-Boltzmann $\quad \overline{W}_{total} = \int_0^{\infty} \overline{W}(\omega) d(\omega) = \frac{\pi^2 k_B^4 T^4}{15 c^3 \hbar^3}$

Strahlungsfeld
Fluktuationen im thermischem Strahlungsfeld

Verteilung der Photonzahl in einer Mode

$$U = \frac{\bar{n}}{1+\bar{n}}$$

$$P_n = \frac{\bar{n}^n}{(1+\bar{n})^n}$$

Fluktuationen der Photonzahl

$$(\Delta n)^2 = \sum_n (n-\bar{n})^2 P_n$$

$$(\Delta n)^2 = \overline{n^2} - (\bar{n})^2 = 2(\bar{n})^2$$

$$\Delta n = \sqrt{(\bar{n})^2 + \bar{n}}$$

für $\bar{n}\alpha >> 1$

$$\Delta n = \bar{n} + \frac{1}{2}$$

n=0 hat die größte Wahrscheinlichkeit

$$P(n=0) = \frac{1}{(1+\bar{n})}$$

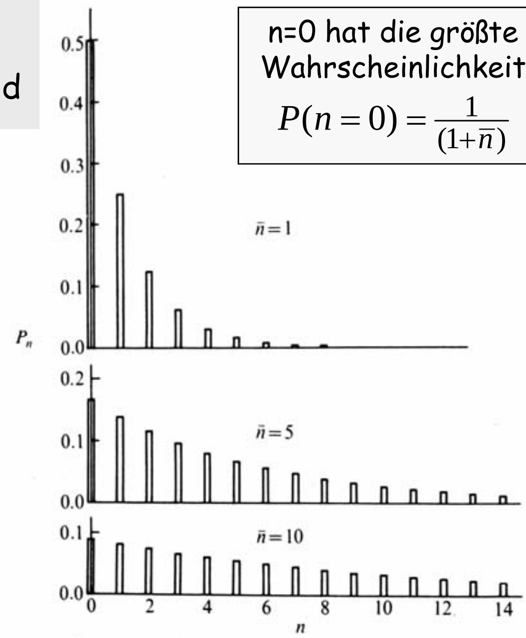

FIG. 1.7. Planck photon-number distributions for three values of the average number $\bar{n}$.

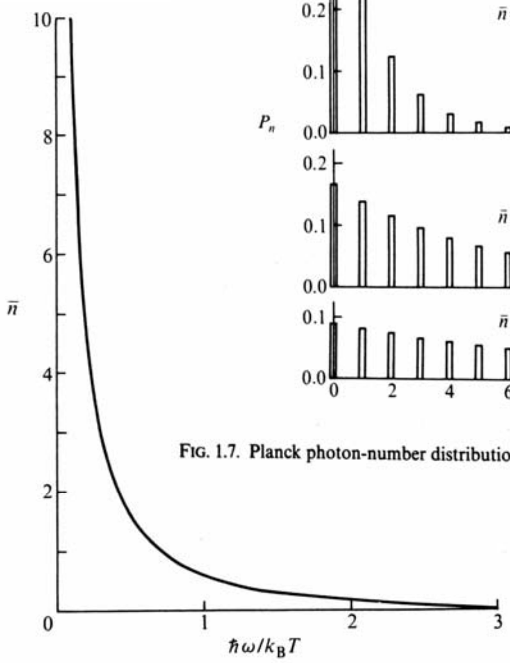

FIG. 1.5. Mean number $\bar{n}$ of photons of frequency ω that are thermally excited at temperature T.

Photonen pro Mode

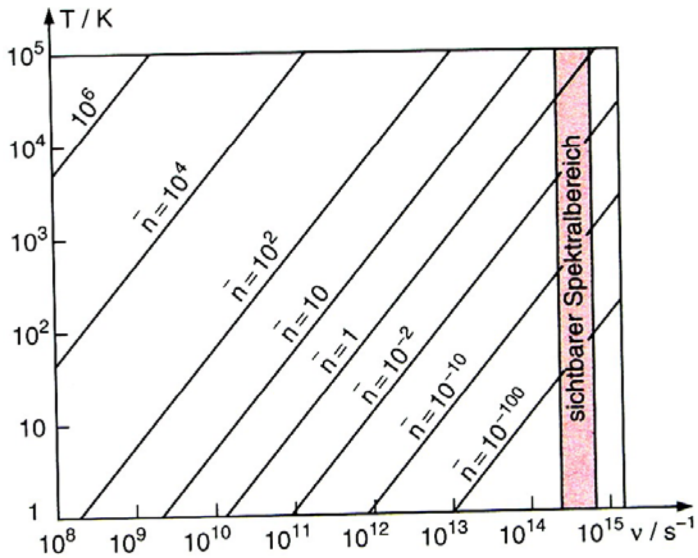

Abb. 7.2. Mittlere Photonenzahl $\bar{n}$ pro Mode des Strahlungsfeldes im thermischen Gleichgewicht als Funktion von Temperatur T und Frequenz ν

Radiation Field

Rate equations and Einstein relations

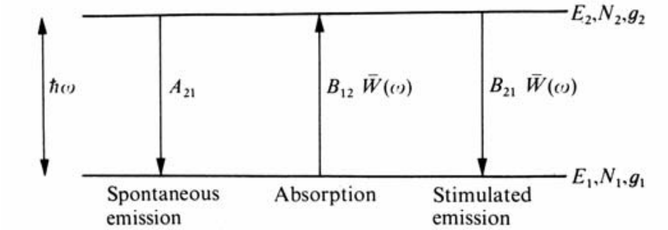

FIG. 1.8. The three basic kinds of radiative process.

$$
\begin{aligned}
\frac{g_1}{g_2} B_{12} &= B_{21} \\
\frac{\hbar\omega^3}{\pi^2 c^3} B_{21} &= A_{21} \\
A_{21} &= \frac{\hbar\omega_0^3 g_1}{\pi^2 c^3 g_2} B_{21} \\
&= \frac{e\omega_0^3 g_1}{3\pi\varepsilon_0 \hbar c^3 g_2} \left|D_{12}\right|^2
\end{aligned}
$$

Quantisierung einer Schwingung
Harmonischer Oszillator

- Energie einer Schwingung ist quantisiert ($\Delta E=\hbar\omega$)
- Schwingungen: Harmonischem Oszillator
- Grundzustandsenergie ($E_0=1/2\ \hbar\omega$): Niedrigster Energiezustand einer Schwingung $E_0=1/2\ \hbar\omega$

→ **Vakuum Fluktuationen**
Vakuum Energie

- Beispiel: Eine elektromagnetische Welle mit Energie 9/2 $\hbar\omega$ enthält 4 Photonen der Frequenz $\nu=\omega/2\pi$

!!!! ACHTUNG !!!!

nicht zu verwechseln mit einem einzelnen Teilchen im 4. angeregten Zustand eines harmonischen Potenzials

Das Korrepondenzprinzip

Klassische Mechanik entsteht als der ‚klassische Limes' der Quantenmechanik.

Klassische Mechanik ist eine ausreichend gute Beschreibung der Natur wenn die von der Quantenmechanik vorhergesagten statistischen Verteilungen der physikalischen Variablen vernachlässigt werden können.

Ehrenfests Theorem:
Die statistischen mittel der Quanten-variablen erfüllen die gleichen Bewegungsgleichungen wie die korrespondierenden klassischen Variablen.

Beispiele:
- Wellenpaket (<x>, <p>)
- Kugel im harmonischen Oszillator (WP in harmon. Osz.)
- Laserlicht

Warnung:
Klassische Zustände sind immer Überlagerungen von vielen Eigenzuständen. Siehe zum Beispiel ein Wellenpaket im harmonischen Oszillator (Überlagerung von vielen Eigenzuständen des HOsz.

‚Reine' Zustände mit ‚großer Quantenzahl' (hoher Anregung) sind meist sehr Quantenmechanisch

Harmonischer Oszillator
große Quantenzahlen

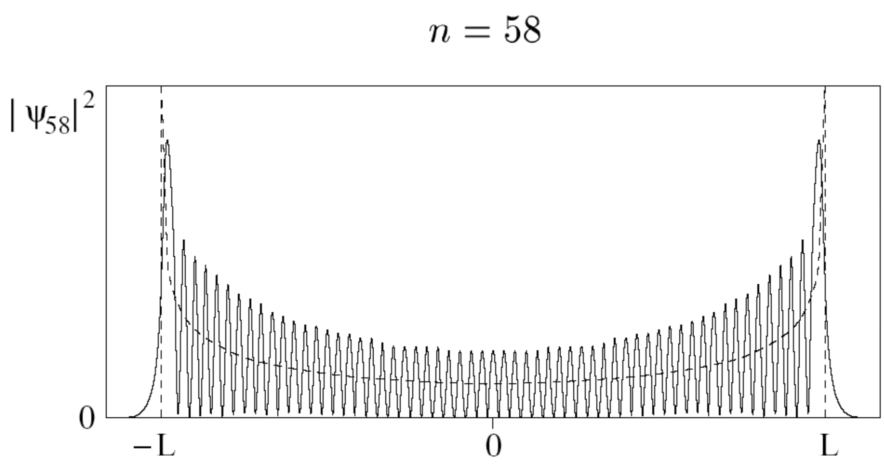

$(n+1)$ Maxima für $|\psi_n|^2$

Hauptmaxima außen: Ozsillation um die *klassisch* zu erwartende Aufenthaltswahrscheinlichkeit eines schwingenden Systems (maximal an den Umkehrpunkten $x = \pm L$)

⇒ *Bohrsches Korrespondenzprinzip:* Übergang zur klassischen Physik im Grenzfall sehr hoher Quantenzahlen

Klassischer Zustand im harmon. Osz.

Wellenpaket:
"klassischer" Zustand

$$|\alpha\rangle = e^{-\frac{1}{2}|\alpha|^2} \sum \frac{\alpha^n}{\sqrt{n!}} |n\rangle$$

Wahrscheinlichkeit für |n>

$$P(n) = e^{-|\alpha|^2} \sum \frac{|\alpha|^{2n}}{n!}$$

Erwartungswert

$$E(n) = |\alpha|^2$$

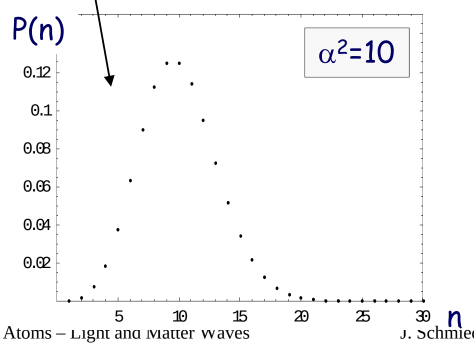

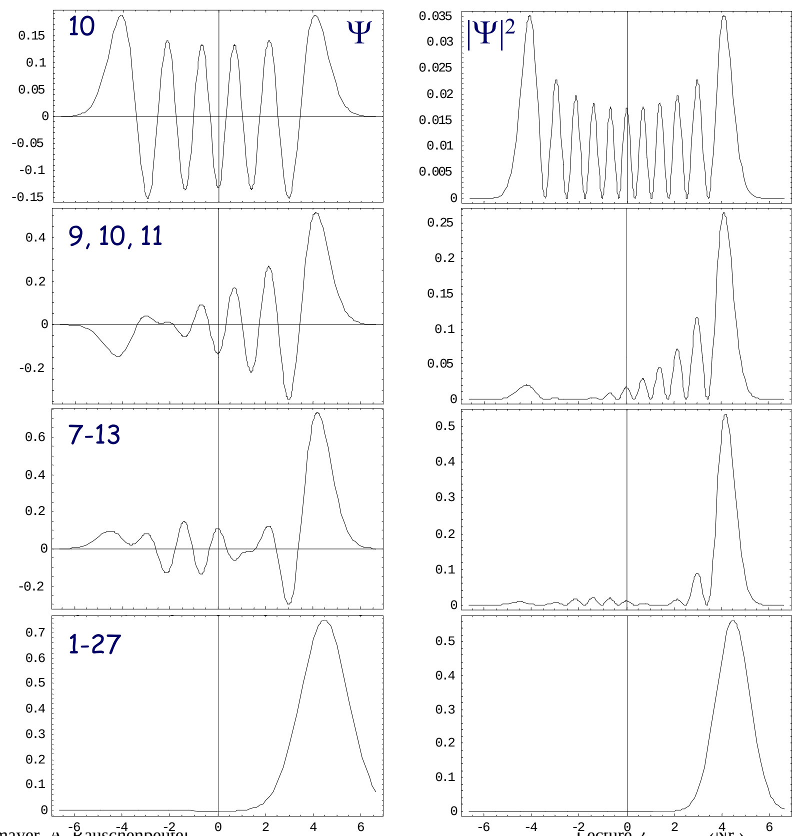

Radiation Field

coherent field

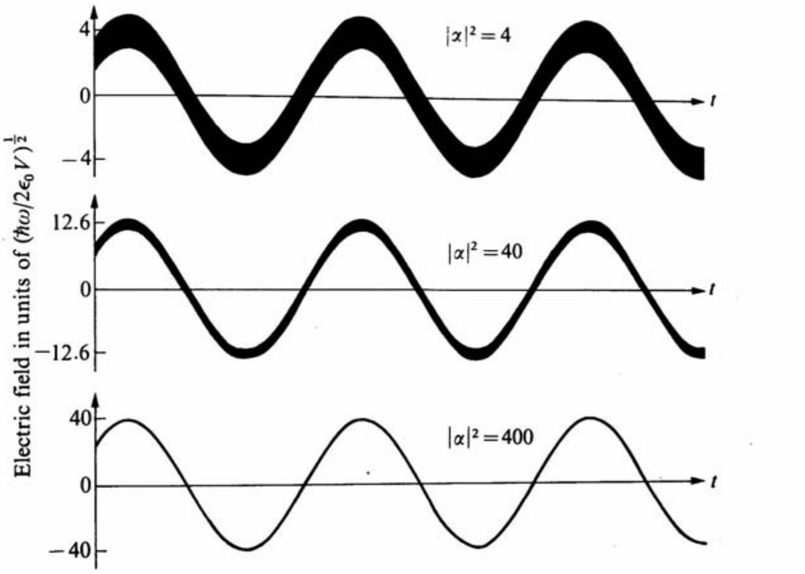

FIG. 4.3. Pictorial representation of the electric-field variation in a cavity mode excited to state $|\alpha\rangle$. Three different values of the mean photon number $|\alpha|^2$ are shown, the vertical scales being different for the three cases. The uncertainties in field values are indicated by the vertical widths $2\Delta E$ of the sine waves. These widths can also be regarded as combinations of the amplitude uncertainty associated with Δn and the phase uncertainty associated with $\Delta \cos \phi$.

Polariation: 2-State-System

Superposition und Basis States

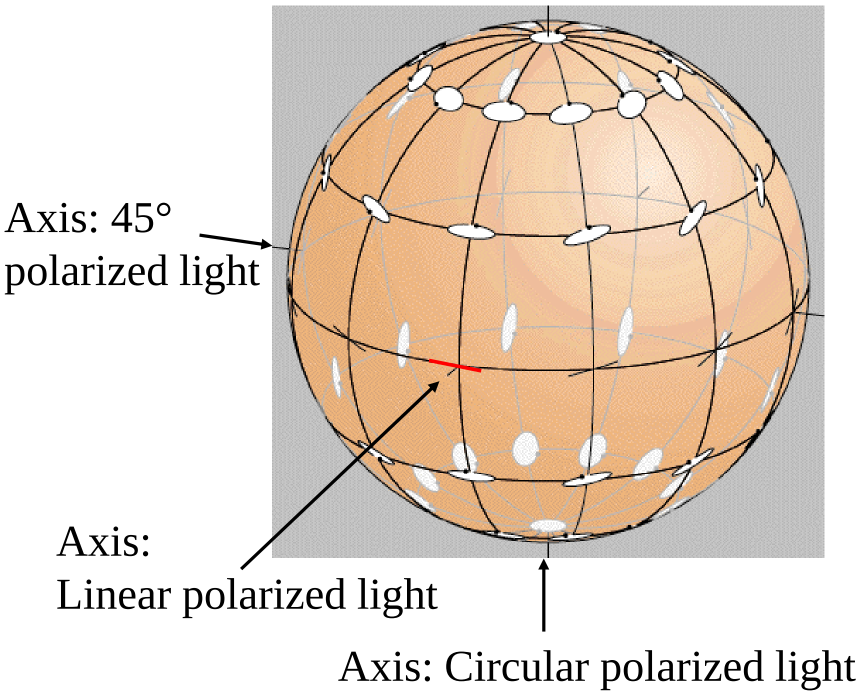

Quanten Bit
2-Zustand-System

Quanten Bit

Superposition

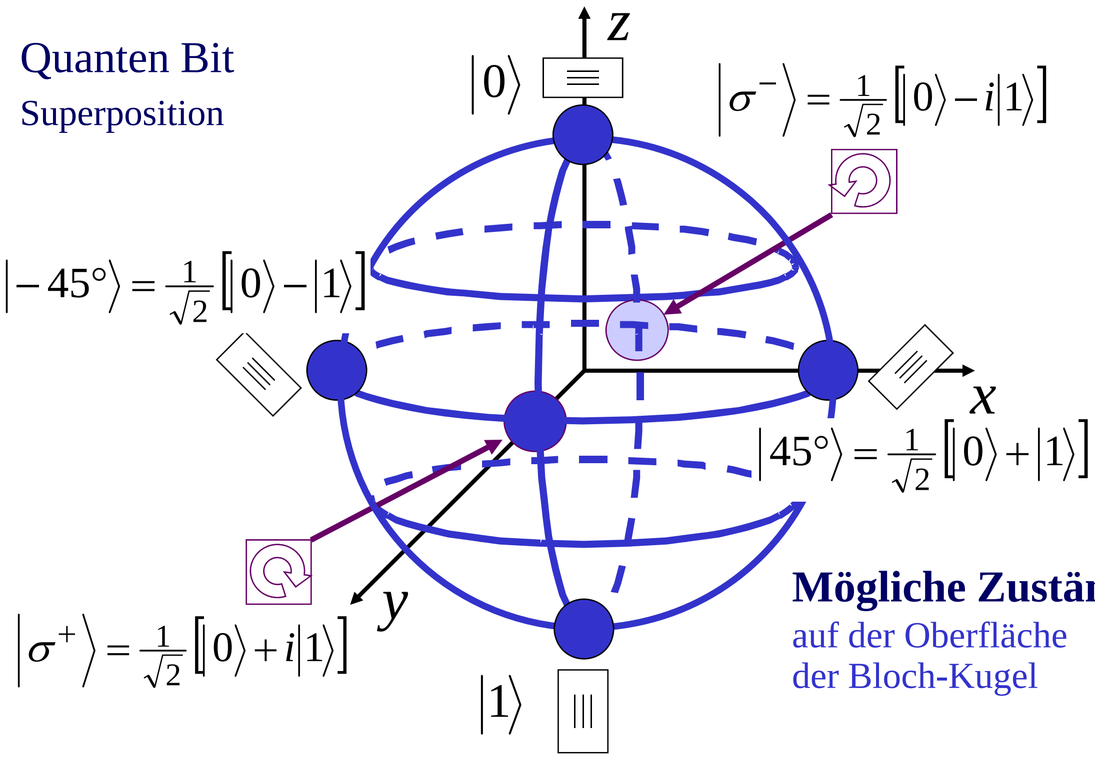

Mögliche Zustände:

auf der Oberfläche
der Bloch-Kugel

3. Atom-Light

3.1. QM two level system formal (level repulsion)
3.2. QM Atom-Light (Chapter 2 Loudon)
 3.2.1. The rotating wave approximation
 3.2.2. Rotating frames
3.3. The Optical Bloch equations
3.4. Alternative: Quantum Monte Carlo

Coupled Two Level System I

Phys. Rev. A 23, 3107 (1981)

II. THEORY OF NONADIABATIC TRANSITIONS AT AN AVOIDED CROSSING

A. The Landau-Zener effect

Before discussing dynamical behavior at an avoided crossing in detail, it is helpful to recapitulate the important features of the theory. We are concerned with a system whose Hamiltonian depends on some variable parameter q, such as the internuclear separation between two atoms or the amplitude of an applied electric or magnetic field. Of particular interest are two eigenstates of the system whose energy levels, to first approximation, cross for some value of q, as in Fig. 1(a).

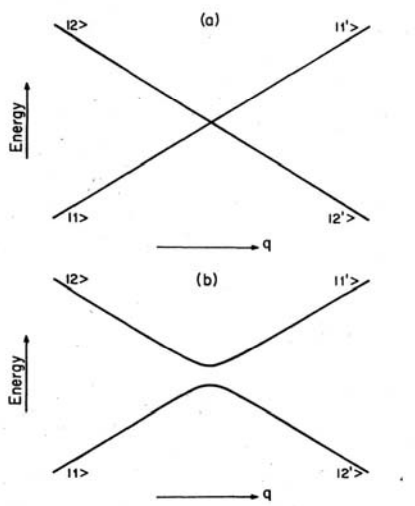

FIG. 1. Energy of the two-level system as a function of the parameter q. (a) Unperturbed energies. (b) An avoided crossing.

If the Hamiltonian is perturbed by an interaction $\mathcal{V}$ which couples the levels, the degeneracy at the crossing is broken. The levels repel, as in Fig. 1(b), in accordance with the "no-crossing" theorem.[7]

Consider a system initially prepared in state $|2\rangle$ of Fig. 1(b). If q then increases in time, sweeping the energies through the avoided crossing, will the system emerge in state $|2'\rangle$, or in state $|1'\rangle$? For the simplest case, where the unperturbed energy separation $E=E_1-E_2$ varies linearly with q, as in Fig. 1(a), and q changes linearly with time, then the probability that the system will undergo a transition to $|2'\rangle$ is

$$P=\exp\left(-2\pi\frac{|\mathcal{V}_{12}|^2}{\hbar(dE/dt)}\right). \quad (1)$$

Here $\mathcal{V}_{12}$ is the matrix element of $\mathcal{V}$ connecting the two states, and $dE/dt=(dE/dq)(dq/dt)$ is the slew rate. It is evident that the behavior at the avoided crossing depends on the slope of the energy levels and the rate at which q changes compared to $|\mathcal{V}_{12}|$. In the limit $\mathcal{V}_{12}\to 0$, $P\to 1$, and the crossing is said to be traversed diabatically. In the opposite limit where $|\mathcal{V}_{12}|^2/h$ is very large compared to the slew rate $P\to 0$ and the avoided crossing is said to be traversed adiabatically. Of more general interest is the intermediate case in which the behavior is neither purely adiabatic nor purely diabatic.

B. Dynamical equations

We consider a two-level system governed by a Hamiltonian $\hbar H_0(q)$ which depends explicitly on a parameter q. Denoting the eigenfunctions of $\hbar H_0$ by $|1\rangle$, $|2\rangle$, and expressing energies in frequency units, we have

Coupled Two Level System II

Phys. Rev. A 23, 3107 (1981)

$$H_0(q)\,|1\rangle = \Omega_1(q)\,|1\rangle\,, \tag{2a}$$

$$H_0(q)\,|2\rangle = \Omega_2(q)\,|2\rangle\,, \tag{2b}$$

where $\Omega_{1,2}(q)$ are the eigenenergies. We assume that the eigenvectors $|1\rangle$, $|2\rangle$ do not vary with q, and that $H_0(q)$ possesses a symmetry which permits degeneracy of the energy levels at some value of q. In the vicinity of the crossing, the energy levels are taken to vary linearly with q, as shown by the dashed lines in Fig. 2.

Next we consider the effect of a perturbation V which lacks the symmetry of H_0 and breaks the degeneracy at the crossing. The total Hamiltonian is

$$\hbar H = \hbar H_0 + \hbar V\,. \tag{3}$$

The matrix of H in the ordered basis $\{|1\rangle, |2\rangle\}$ is

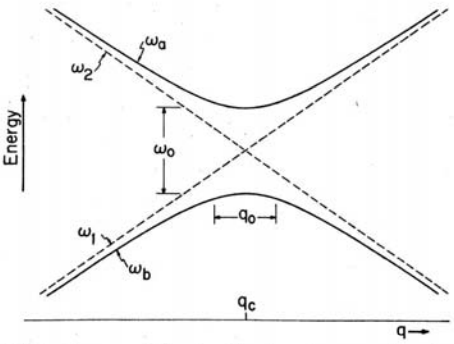

FIG. 2. Energy of the two-level system as a function of the parameter q. The dashed lines are the diagonal energies of H, and the solid lines are its eigenenergies.

$$H(q) = \begin{pmatrix} \omega_1(q) & \frac{1}{2}\omega_0 e^{-i\phi} \\ \frac{1}{2}\omega_0 e^{i\phi} & \omega_2(q) \end{pmatrix}, \tag{4}$$

where

$$\omega_1(q) = \Omega_1(q) + \langle 1\,|\,V\,|1\rangle\,, \tag{5a}$$

$$\omega_2(q) = \Omega_2(q) + \langle 2\,|\,V\,|2\rangle\,, \tag{5b}$$

$$\tfrac{1}{2}\omega_0 = |\langle 1\,|\,V\,|2\rangle|\,, \tag{5c}$$

$$\langle 1\,|\,V\,|2\rangle = \tfrac{1}{2}\omega_0 e^{-i\phi}\,, \quad 0 \le \phi < 2\pi\,. \tag{5d}$$

We assume that V is independent of q so that ω_0 is a constant. The diagonal matrix elements of V shift the location of the crossing but do not affect the dynamics of the system.

The eigenenergies of H are

$$\omega_a(q) = \tfrac{1}{2}\{(\omega_1 + \omega_2) + [\omega(q)^2 + \omega_0^2]^{1/2}\}\,, \tag{6a}$$

$$\omega_b(q) = \tfrac{1}{2}\{(\omega_1 + \omega_2) - [\omega(q)^2 + \omega_0^2]^{1/2}\}\,, \tag{6b}$$

where $\omega(q) = \omega_1 - \omega_2$. The "crossing value" of the parameter, q_c, is defined by $\omega(q_c) = 0$. The energies (in frequency units) are shown by the solid lines in Fig. 2. The avoided crossing can be characterized by its separation, ω_0, and its width q_0 defined by

$$q_0 = \omega_0 \Big/ \left(\frac{d\omega}{dq}\right)_{q_c}\,. \tag{7}$$

The eigenfunctions of H are conveniently written in terms of the phase angle ϕ [Eq. 5(d)] and the parameter θ defined by

$$\tan\theta(q) = \frac{\omega_0}{\omega(q)}\,, \quad 0 \le \theta < \pi\,. \tag{8}$$

A set of orthonormal eigenvectors is

Coupled Two Level System III

Phys. Rev. A 23, 3107 (1981)

$$|a(q)\rangle = \cos\left(\frac{\theta(q)}{2}\right) e^{-i\phi/2}\,|1\rangle + \sin\left(\frac{\theta(q)}{2}\right) e^{i\phi/2}\,|2\rangle\,, \tag{9a}$$

$$|b(q)\rangle = -\sin\left(\frac{\theta(q)}{2}\right) e^{-i\phi/2}\,|1\rangle + \cos\left(\frac{\theta(q)}{2}\right) e^{i\phi/2}\,|2\rangle\,. \tag{9b}$$

$|a(q)\rangle$ and $|b(q)\rangle$ have energies ω_a and ω_b, respectively.

Now let us examine the effect of time variations in q. The time-dependent Schrödinger equation

$$H\,|\Psi(t)\rangle = i\,\frac{\partial\,|\Psi(t)\rangle}{\partial t} \tag{10}$$

may be solved by taking

$$|\Psi(t)\rangle = C_1(t)\exp\left(-i\int_0^t \omega_1 dt'\right)|1\rangle + C_2(t)\exp\left(-i\int_0^t \omega_2 dt'\right)|2\rangle\,. \tag{11}$$

Substituting Eq. (11) into (10) and using (5) results in

$$i\dot{C}_1 = \tfrac{1}{2}\omega_0 e^{-i\phi}\exp\left(i\int_0^t \omega\, dt'\right) C_2\,, \tag{12a}$$

$$i\dot{C}_2 = \tfrac{1}{2}\omega_0 e^{i\phi}\exp\left(-i\int_0^t \omega\, dt'\right) C_1\,. \tag{12b}$$

These may be decoupled to yield

$$\ddot{C}_1 - i\omega(t)\dot{C}_1 + \frac{\omega_0^2}{4} C_1 = 0\,, \tag{13a}$$

$$\ddot{C}_2 + i\omega(t)\dot{C}_2 + \frac{\omega_0^2}{4} C_2 = 0\,. \tag{13b}$$

For a particular initial state, initial values of C_1 and C_2 are determined by Eqs. (8), (9), and (11), and values of $\dot{C}_1$ and $\dot{C}_2$ are given by Eqs. (12).

We are concerned with the behavior of the system over an interval starting at time t_i and ending at time t_f, during which the parameter q changes from q_i to q_f. Assume that the initial state is $|b_i\rangle$, where $b_i = b(q_i)$. The probability that the final state is $|a_f\rangle$, i.e., that the system has "jumped" or made a diabatic transition from $|b\rangle$ to $|a\rangle$, is

$$P = |\langle \Psi(t_f)\,|a_f\rangle|^2\,. \tag{14}$$

If q varies linearly in time, so that $d\omega/dt$ is constant, then Eqs. (13) can be solved.[2] The probability is most conveniently expressed in terms of the parameter

$$\Gamma = \frac{\omega_0^2}{4\left(\frac{d\omega}{dt}\right)} = \frac{|\langle 1\,|\,V\,|2\rangle|^2}{\frac{d\omega}{dt}}\,, \tag{15}$$

where the derivative is evaluated at the crossing. In the limit $t_i \to -\infty$, $t_f \to +\infty$, the result is given by Eq. (1):

$$P = e^{-2\pi\Gamma}\,.$$

Coupled Two Level System

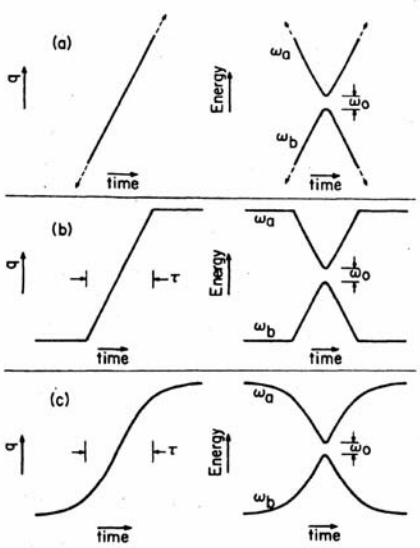

FIG. 3. Possible time variations of q and the corresponding eigenenergies. (a) $q(t)$ linear and extends over all time; the Landau-Zener case. (b) $q(t)$ linear over a finite range; an idealized "fast pulse". (c) $q(t)$ for a more realistic fast pulse; the corresponding $\omega(t)$ is given by Eq. (18).

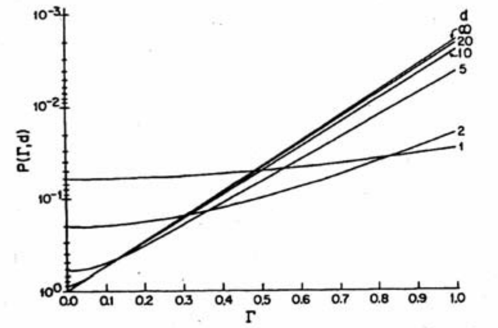

FIG. 4. Diabatic transition probability P as a function of Γ for various values of d. The thin line is the Landau-Zener result ($d=\infty$).

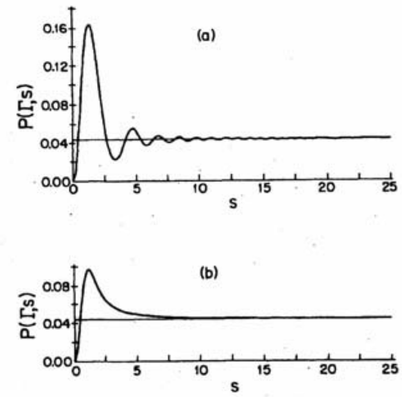

FIG. 5. Diabatic transition probability as a function of s for $\Gamma=0.5$. The thin lines are the Landau-Zener prediction. (a) $q(t)$ given by Fig. 3(b); the "sharp corners" in $q(t)$ produce oscillations. (b) $q(t)$ given by Fig. 3(c).

Coupled Two Level System

Dynamical effects in avoided crossings …

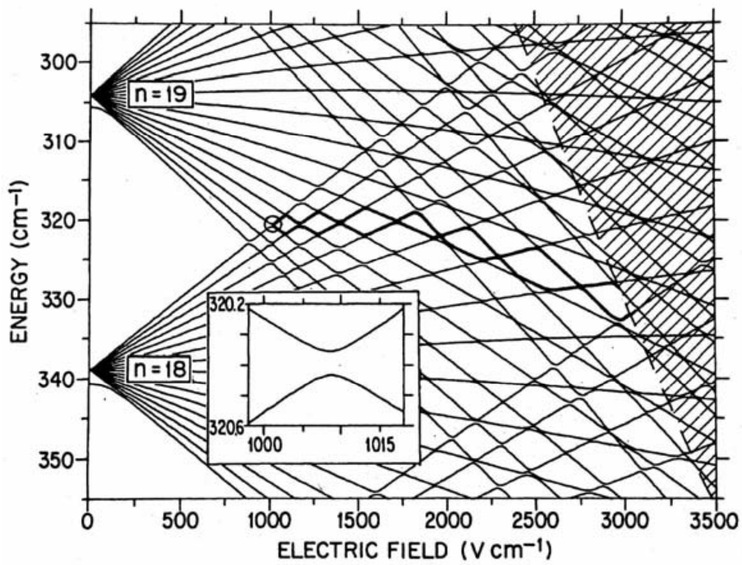

FIG. 6. Stark energies of lithium $|m|=1$ vs electric field. The avoided crossing observed is encircled and shown in detail by the inset. The dashed line is the classical ionization limit (Ref. 15). The heavy lines show the adiabatic path followed by the two states. Avoided crossing sizes are exaggerated by the plotting routine.

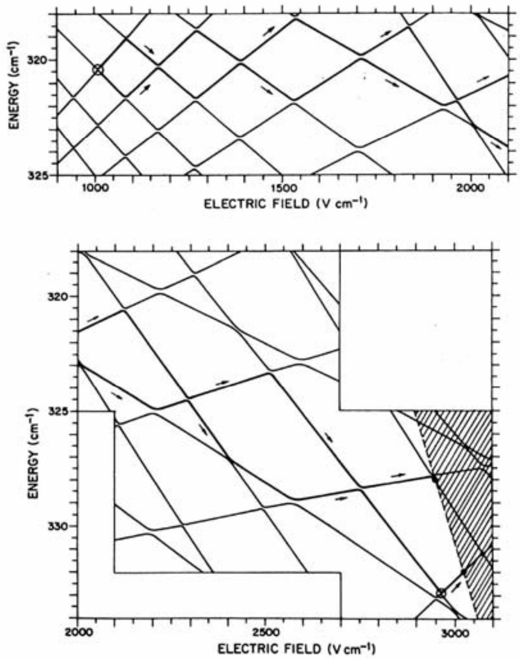

FIG. 9. Details from Fig. 6 of the adiabatic paths followed by the states during pulsed ionization. The avoided crossing sizes are authentic. The circled feature near the ionization limit is discussed in the text.

Coupled Two Level System

Dynamical effects in avoided crossings …

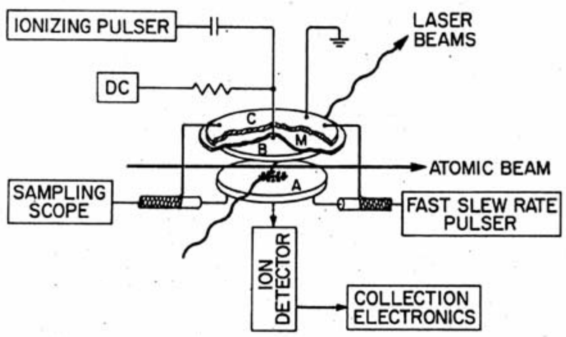

FIG. 7. Schematic diagram of the experimental system. A and B are field plates, C is a ground plane, and M is an insulating Mylar film.

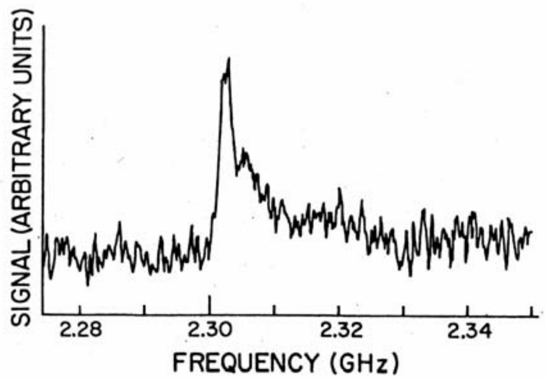

FIG. 8. Resonance curve for the avoided crossing; signal proportional to rf transition probability vs frequency.

Wechselwirkung Atom-Licht

Dipol-Näherung

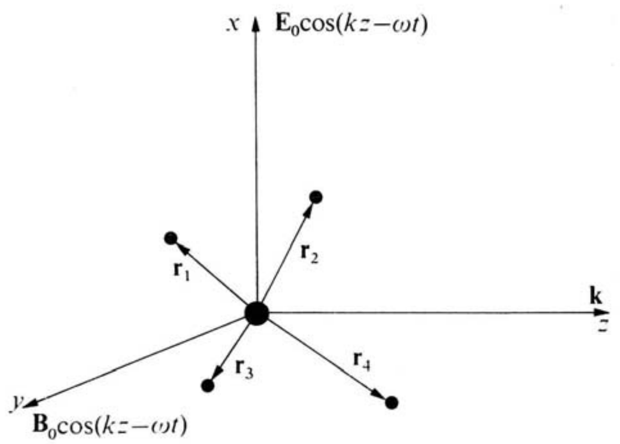

FIG. 2.1. Coordinate system for the atom and the electromagnetic wave.

Dipole matrix elements

The transition matrix elements M_{mj} are given by:

$$\hbar M_{mj} = \int \psi_m^* \hat{H}_i \psi_j dV = \langle \psi_m | \hat{H}_i | \psi_j \rangle$$

with $\hat{H}_i = e\mathbf{D} \cdot \mathbf{E}_0 \cos(\omega t)$

$e\mathbf{D}$ being the total electric dipole.
From symmetry one immediately sees:

$$M_{11} = M_{22} = 0$$
$$M_{12} = M_{21}^* = \frac{1}{\hbar} e E_0 X_{12} \cos(\omega t)$$

where

$$X_{12} = \int \psi_1^* X \psi_2 dV = \langle \psi_1 | X | \psi_2 \rangle$$

is the dipole matrix element. For further on

we define the Rabi frequency $\Omega_{Rabi} = \frac{1}{\hbar} e E_0 X_{12}$

Atom- Licht WW
Beschr. durch Wellenfunktion

We start from the time dependent Schrödinger equation:

$$\hat{H}\Psi(r,t) = i\hbar\frac{d\Psi(r,t)}{dt} \tag{3.1}$$

Let us assume the atom (described by the Hamiltonian $\hat{H}_{Atom}$9 is driven by an external electro magnetic field with frequency $\omega/2\pi$ (interaction Hamiltonian $\hat{H}_i$). The total Hamiltonian $\hat{H}$ is then:

$$\hat{H} = \hat{H}_{Atom} + \hat{H}_i \tag{3.2}$$

For the plane atom (without external drive) the stationary solution for the n-th atomic eigenstate $\psi_n(r)$is given by the time independent Schrödinger equation:

$$\hat{H}_{Atom}\psi_n(r) = E_n\psi_n(r) \tag{3.3}$$

The complete wave function $\Psi_n(r,t)$ is then

$$\Psi_n(r,t) = \exp(-i\frac{E_n t}{\hbar})\psi_n(r) \tag{3.4}$$

In the following we will consider a 2-level system $|\psi_1\rangle$ and $|\psi_2\rangle$ with energy eigen values E_1 and E_2. The energy difference is then related to the transition frequency $\omega_0/2\pi$

$$\hbar\omega_0 = E_2 - E_1 \tag{3.5}$$

Let us assume the two level atom is driven by an external electro magnetic field (frequency $\omega/2\pi$, interaction Hamiltonian $\hat{H}_i$). (total Hamiltonian $\hat{H} = \hat{H}_{Atom} + \hat{H}_i$). The solution to the Schrödinger equation 3.1 can then be written as:

$$\Psi(r,t) = C_1(t)\Psi_1(r,t) + C_2(t)\Psi_2(r,t) \tag{3.6}$$

Atom- Licht WW
Beschr. durch Wellenfunktion

with $|C_1(t)|^2 + |C_2(t)|^2 = 1$. Inserting Eq. 3.6 into Eq. 3.1 and using Eq. 3.3 and Eq. 3.1 and using the orthogonality relation between eigenstates ($\int \psi_m^*\psi_j dV = \delta_{mj}$) one obtains the following equations for the coefficients $C_1(t)$ and $C_2(t)$

$$\begin{aligned} C_1 M_{11} + C_2\exp(-i\omega_0 t)M_{12} &= i\frac{dC_1}{dt} \\ C_1\exp(i\omega_0 t)M_{21} + C_2 M_{22} &= i\frac{dC_2}{dt} \end{aligned} \tag{3.7}$$

where M_{mj} are the transition matrix elements given by:

$$\hbar M_{mj} = \int \psi_m^*\hat{H}_i\psi_j dV = \langle\psi_m|\hat{H}_i|\psi_j\rangle \tag{3.8}$$

Interaction Hamiltonian

The main contribution to the interaction Hamiltonian $\hat{H}_i$ arises then from the potential energy hat the induced electric dipole $e\mathbf{D} = e\sum r_j$ feels in the driving field $E_0\cos\omega t$.

$$\hat{H}_i = e\mathbf{D}\cdot\mathbf{E}_0\cos(\omega t) \tag{3.9}$$

From symmetry (The dipole interaction Hamiltonian $\hat{H}_i$ has odd symmetry when changing r to $-r$) one immediately sees:

$$\begin{aligned} M_{11} &= M_{22} = 0 \\ M_{12} &= M_{21}^* = \frac{1}{\hbar}eE_0X_{12}\cos(\omega t) \end{aligned} \tag{3.10}$$

where

$$X_{12} = \int \psi_1^* X\psi_2 dV = \langle\psi_1|X|\psi_2\rangle \tag{3.11}$$

is the dipole matrix element. For further on we define the Rabi frequency Ω_{Rabi} as

$$\Omega_{Rabi} = \frac{1}{\hbar}eE_0X_{12} \tag{3.12}$$

Rabi Oszillationen

Using these matrix elements the above equations (Eq.3.7) can be now written as:

$$\begin{aligned}\Omega_{Rabi}\cos(\omega t)\exp(-i\omega_0 t)C_2 &= i\frac{dC_1}{dt} \\ \Omega^*_{Rabi}\cos(\omega t)\exp(i\omega_0 t)C_1 &= i\frac{dC_2}{dt}\end{aligned} \tag{3.13}$$

the time dependent terms $\cos(\omega t)\exp(-i\omega_0 t)$ can be rewritten using $\cos(\omega t) = \frac{1}{2}(e^{i\omega t}+e^{-i\omega t})$ as:

$$\cos(\omega t)\exp(-i\omega_0 t) = \frac{1}{2}\left(\exp(-i(\omega-\omega_0)t) + \exp(-i(\omega+\omega_0)t)\right) \tag{3.14}$$

for $|\omega - \omega_0| \ll \omega$ we can neglect the fast oscillating terms $(\omega+\omega_0)t$. The evolution will be governed by the slow oscillating terms. This approximation is called the **Rotating Wave Approximation (RWA)**.

$$\begin{aligned}\Omega_{Rabi}\frac{1}{2}\exp(-i(\omega-\omega_0)t)C_2 &= i\frac{dC_1}{dt} \\ \Omega^*_{Rabi}\frac{1}{2}\exp(i(\omega-\omega_0)t)C_1 &= i\frac{dC_2}{dt}\end{aligned} \tag{3.15}$$

for zero detuning: $\omega = \omega_0$ one finds then the well known **Rabi oscillations** between the ground and excited state of the driven two level system. With the starting conditions $|C_1|^2 = 1$ and $|C_2|^2 = 0$ one finds:

$$\begin{aligned}|C_1|^2 &= \cos^2(\Omega_{Rabi}t/2) \\ |C_2|^2 &= \sin^2(\Omega_{Rabi}t/2)\end{aligned} \tag{3.16}$$

Equations 3.13 provide an exact description of the state of a two level atom (without decay) interacting with an oscillating electric field. But for general solution, and because the interesting quantities are not the bare coefficients C_i but the probabilities $|C_i|^2$ they are best transformed into equations for the density matrix.

In addition it is not simple to include the decay of the excited state in the wave function description of the atom-light interaction.

Optische Bloch Gleichungen

Beschreibung durch die Dichtematrix

From the coefficients C_1 and C_2 we can form equations for the density matrix of the atom:

$$\begin{aligned}\rho_{11} &= |C_1|^2 = \frac{N_1}{N} \\ \rho_{22} &= |C_2|^2 = \frac{N_2}{N} \\ \rho_{12} &= C_1 C_2^* \\ \rho_{21} &= C_2 C_1^*\end{aligned} \tag{3.17}$$

with the diagonal elements ρ_{11} and ρ_{22} satisfying

$$\rho_{11} + \rho_{22} = 1 \tag{3.18}$$

and the off diagonal matrix elements are in general complex and they satisfy

$$\rho_{12} = \rho^*_{21} \tag{3.19}$$

Optische Bloch Gleichungen

Ohne spontane Emission

One can find the equations of motion for the density matrix easily from the equations of motion of the coefficients C_1 and C_2 equation 3.13

$$\frac{d\rho_{22}}{dt} = -\frac{d\rho_{11}}{dt} = -i\cos(\omega t)\left[\Omega^*_{Rabi}\exp(i\omega_0 t)\rho_{12} - \Omega_{Rabi}\exp(-i\omega_0 t)\rho_{21}\right] \quad (3.20)$$

$$\frac{d\rho_{12}}{dt} = +\frac{d\rho^*_{21}}{dt} = +i\Omega_{Rabi}\cos(\omega t)\exp(-i\omega_0 t)(\rho_{11}-\rho_{22})$$

apply the **rotating wave approximation**: $(|\Delta| = |\omega - \omega_0| \ll \omega_0)$

$$\frac{d\rho_{22}}{dt} = -\frac{d\rho_{11}}{dt} = -\frac{1}{2}i\Omega^*_{Rabi}\exp(i(\omega_0-\omega)t)\rho_{12} + \frac{1}{2}i\Omega_{Rabi}\exp(-i(\omega_0-\omega)t)\rho_{21} \quad (3.21)$$

$$\frac{d\rho_{12}}{dt} = -+\frac{d\rho^*_{21}}{dt} = +\frac{1}{2}i\Omega_{Rabi}\exp(-i(\omega_0-\omega)t)(\rho_{11}-\rho_{22})$$

These can be solved using the Ansatz:

$$\begin{aligned}\rho_{11} &= \rho^{(0)}_{11}\exp(\lambda t) \quad (3.22)\\ \rho_{22} &= \rho^{(0)}_{22}\exp(\lambda t)\\ \rho_{12} &= \rho^{(0)}_{12}\exp(-i(\omega_0-\omega)t)\exp(\lambda t)\\ \rho_{21} &= \rho^{(0)}_{21}\exp(-i(\omega_0-\omega)t)\exp(\lambda t)\end{aligned}$$

Optische Bloch Gleichungen

Ohne spontane Emission

which leads to the following equation:

$$\begin{bmatrix} -\lambda & 0 & \frac{1}{2}i\Omega^*_{Rabi} & -\frac{1}{2}i\Omega_{Rabi} \\ 0 & -\lambda & -\frac{1}{2}i\Omega^*_{Rabi} & \frac{1}{2}i\Omega_{Rabi} \\ \frac{1}{2}i\Omega_{Rabi} & -\frac{1}{2}i\Omega_{Rabi} & i(\omega_0-\omega)-\lambda & 0 \\ -\frac{1}{2}i\Omega^*_{Rabi} & \frac{1}{2}i\Omega^*_{Rabi} & 0 & -i(\omega_0-\omega)-\lambda \end{bmatrix} \cdot \begin{bmatrix} \rho^{(0)}_{11} \\ \rho^{(0)}_{22} \\ \rho^{(0)}_{12} \\ \rho^{(0)}_{21} \end{bmatrix} = 0 \quad (3.23)$$

and the following eigen value equation:

$$\lambda^2[\lambda^2 + (\omega_0-\omega)^2 + |\Omega_{Rabi}|^2] = 0 \quad (3.24)$$

with the solutions:

$$\begin{aligned}\lambda_1 &= 0 \quad (3.25)\\ \lambda_2 &= i\Omega\\ \lambda_3 &= -i\Omega\end{aligned}$$

thereby we used

$$\Omega = \sqrt{(\omega_0-\omega)^2 + |\Omega_{Rabi}|^2]} \quad (3.26)$$

Optische Bloch Gleichungen

Ohne spontane Emission

The general solution is then:

$$\rho_{ij} = \rho_{ij}^{(1)} + \rho_{ij}^{(2)} \exp(i\Omega t) + \rho_{ij}^{(3)} \exp(-i\Omega t) \tag{3.27}$$

For the special initial conditions:

$$\begin{aligned} \rho_{11} &= 1 \\ \rho_{22} &= 0 \\ \rho_{12} &= \rho_{21} = 0 \end{aligned} \tag{3.28}$$

one finds:

$$\begin{aligned} \rho_{22}(t) &= \frac{|\Omega_{Rabi}|^2}{\Omega^2} \sin^2\left(\frac{1}{2}\Omega t\right) \qquad (3.29) \\ \rho_{12}(t) &= \exp(-i(\omega_0 - \omega)t) \frac{\Omega_{Rabi}}{\Omega^2} \sin\left(\frac{1}{2}\Omega t\right) \left(-(\omega_0 - \omega) \sin\left(\frac{1}{2}\Omega t\right) + i\Omega \cos\left(\frac{1}{2}\Omega t\right)\right) \end{aligned}$$

and for resonant light ($\omega_0 = \omega$) the solutions become even simpler:

$$\begin{aligned} \rho_{22}(t) &= \sin^2(\frac{1}{2}\Omega_{Rabi} t) \\ \rho_{12}(t) &= \frac{\Omega_{Rabi}}{|\Omega_{Rabi}|} \sin(\frac{1}{2}\Omega_{Rabi} t) \cos(\frac{1}{2}\Omega_{Rabi} t) \end{aligned} \tag{3.30}$$

Optical Bloch Equation

without radiation damping

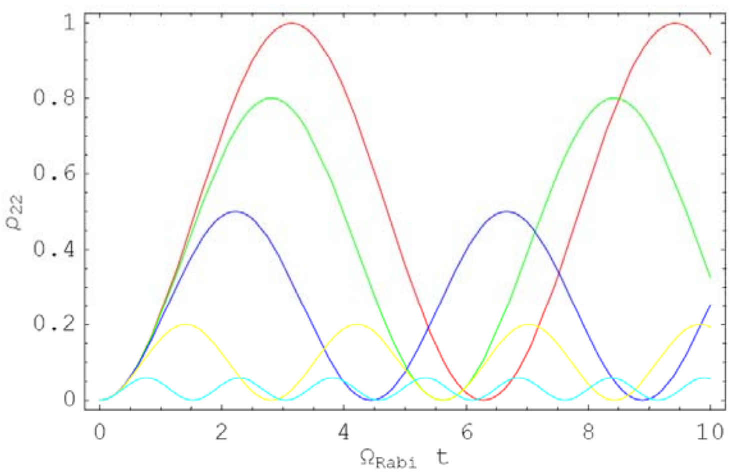

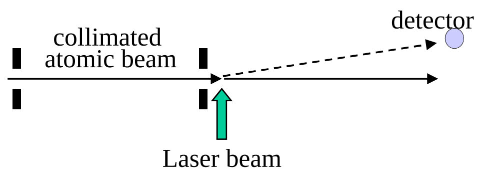

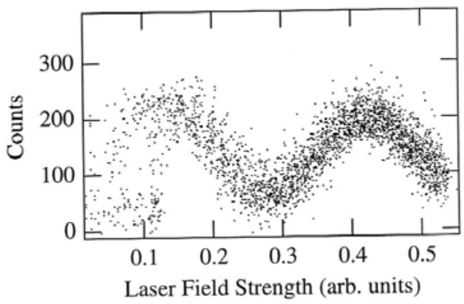

Figure 8: Using Rabi flops in momentum transfer: The detector is displaced from the collimation axis by one photon recoil, and we measure the count rate as a function of laser intensity. As the power increases, the atoms have an oscillatory probability of being excited that is given by the Rabi formula. To scatter a single photon, we set the power to the value at the first maximum of these oscillations, which closely corresponds to a _-pulse.

Optische Bloch Gleichungen
mit spontaner Emission

Apply the rotating wave approximation: ($|\Delta| = |\omega - \omega_0| \ll \omega_0$)

$$\frac{d\rho_{22}}{dt} = -\frac{d\rho_{11}}{dt} = -\frac{1}{2} i\Omega^*_{Rabi} \exp(i(\omega_0 - \omega)t)\rho_{12} + \frac{1}{2} i\Omega_{Rabi} \exp(-i(\omega_0 - \omega)t)\rho_{21} - 2\gamma\rho_{22}$$
$$\frac{d\rho_{12}}{dt} = +\frac{d\rho^*_{21}}{dt} = +\frac{1}{2} i\Omega_{Rabi} \exp(-i(\omega_0 - \omega)t)(\rho_{11} - \rho_{22}) - \gamma\rho_{12} \qquad (3.31)$$

only in the case of resonant light ($\omega_0 = \omega$) we can give a general solution: for the special initial conditions:

$$\rho_{11} = 1, \quad \rho_{22} = 0, \quad \rho_{12} = \rho_{21} = 0 \qquad (3.32)$$

one finds:

$$\rho_{22} = \frac{\frac{1}{2}|\Omega_{Rabi}|^2}{2\gamma^2 + |\Omega_{Rabi}|^2} \left(1 - \left(\cos(\lambda t) + \frac{3\gamma}{2\lambda}\sin(\lambda t)\right) \exp\frac{3\gamma}{2\lambda}\right) \qquad (3.33)$$

with

$$\lambda = \sqrt{|\Omega_{Rabi}|^2 + \frac{1}{2}\gamma^2} \qquad (3.34)$$

in general there are no closed solutions for these equations 3.31. So let's first look at the steady state solutions:

$$\rho_{22} = \frac{\frac{1}{4}|\Omega_{Rabi}|^2}{(\omega_0 - \omega)^2 + \gamma^2 + \frac{1}{2}|\Omega_{Rabi}|^2} \qquad (3.35)$$
$$\rho_{12} = \exp(-i(\omega_0 - \omega)t)) \frac{\frac{1}{2}|\Omega_{Rabi}|(\omega_0 - \omega - i\gamma)}{(\omega_0 - \omega)^2 + \gamma^2 + \frac{1}{2}|\Omega_{Rabi}|^2}$$

Optical Bloch Equation
with radiation damping

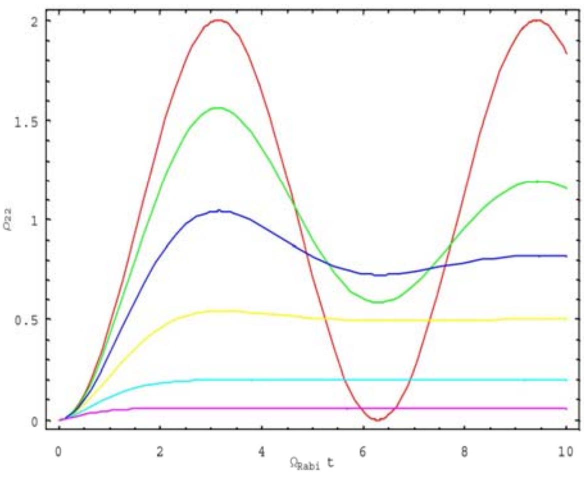

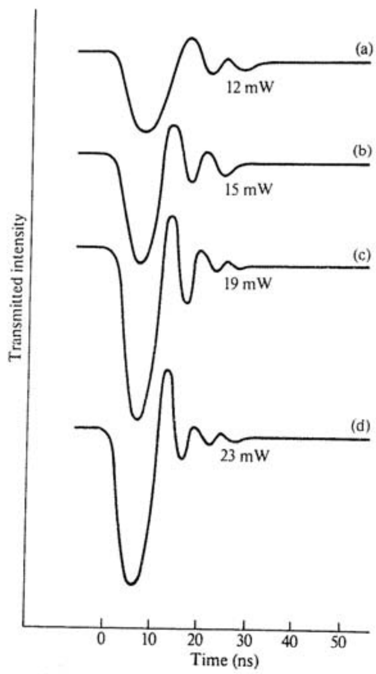

FIG. 2.8. Intensity of light transmitted through sodium vapour as a function of laser power. (After W. R. MacGillivray *et al.*, ref. 8.)

Line Shape

power broadening

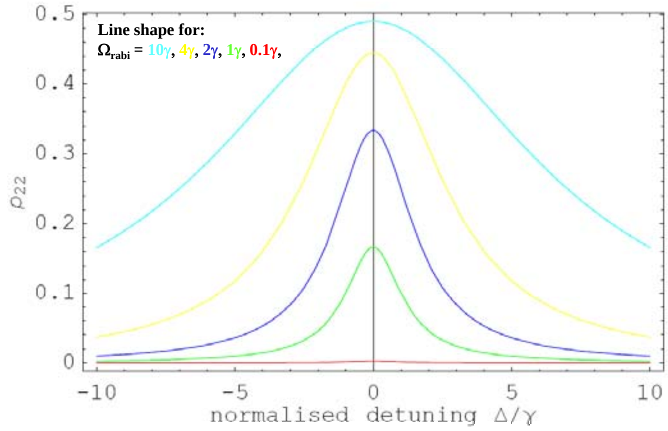

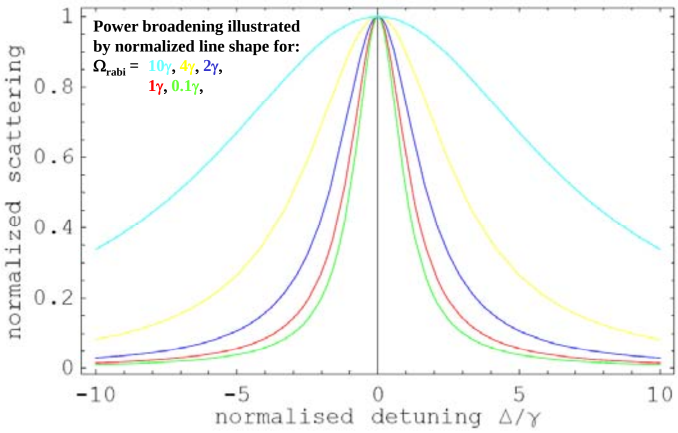

Doppler broadening

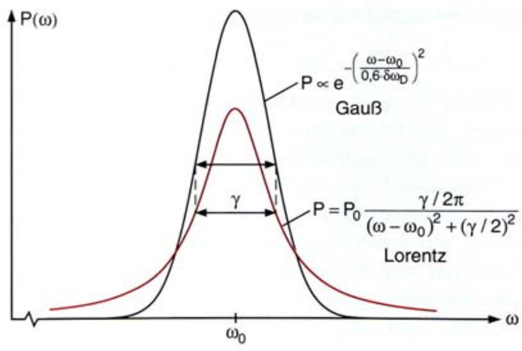

Abb. 7.20. Vergleich von Lorentzprofil und Gaußprofil mit gleicher Halbwertsbreite

Normalized Lorenzian line shape:
width: FWHM = 2γ

Doppler boadening:
line shape ⇨ Gaussian
width: $\sigma \sim k v_{mean}$

$$\sigma = \frac{\omega_0}{c}\sqrt{\frac{k_B T}{M}}$$

Damped resonance in a classical system

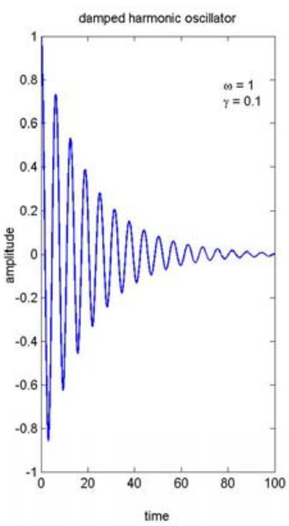

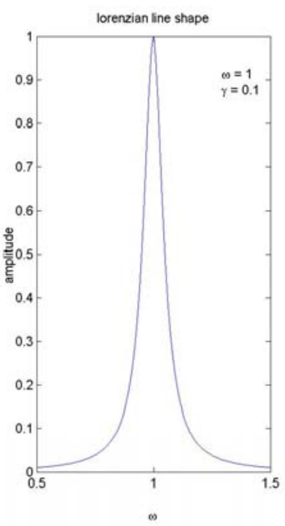

Harmonic oszillator (RLC circuit):

The charge q obeys: $\ddot{q} + \gamma\dot{q} + \omega_0^2\gamma = 0$

with $\gamma = R/L, \omega_0^2 = 1/LC$

Solution is a linear combination of

$$\exp\left(-\frac{\gamma}{2}\right)\exp(\pm i\omega' t)$$

with $\omega' = \omega_0\sqrt{1-\gamma^2/4\omega_0^2}.$

For ω>>γ we find ω'= ω and the energy in the circuit is

$$W = \frac{1}{2C}q^2 + \frac{1}{2}L\dot{q}^2 = \omega_0 e^{-\gamma t}$$

If the circuit is periodically driven by voltage E_0 at frequency ω

$$q_0 = \frac{E_0}{2\omega_0 L}\frac{1}{(\omega_0 - \omega + i\gamma/2}.$$

Magnetic Resonance

exact resonance

Spin in magnetic field: $W = -\vec{\mu}\cdot\vec{B}$

$$\vec{F} = -\nabla W = \nabla(\vec{\mu}\cdot\vec{B})$$

$$\text{torque} = \vec{\mu}\times\vec{B}$$

a)

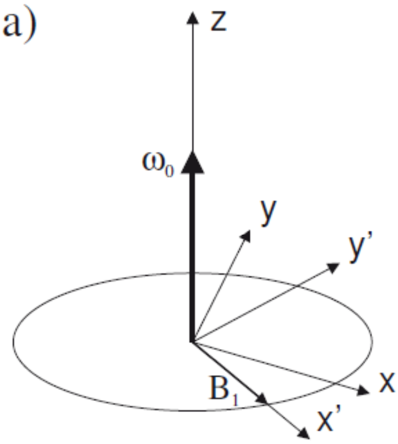

Rotating magnetic field

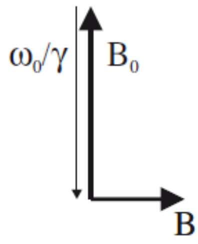

Effective field in the rotating coordinate system

Torque: $\frac{d\vec{J}}{dt} = \gamma\vec{J}\times\vec{B} = -\gamma\vec{B}\times\vec{J}$

Larmor precession $\Omega_L = -\gamma B$

Add a magnetic field B_1 rotating in x-y plane with the Larmor frequency

$$\omega_0 = -\gamma B_0$$

$$\vec{B}(t) = B_1(\hat{x}\ \cos\ \omega_0 t - \hat{y}\ \sin\ \omega_0 t)\ +\ B_0\ \hat{z}.$$

In a coordinate system rotating with ω_0 the magnetic moment sees an effective field

$$\begin{aligned}\vec{B}(t)_{eff} &= \vec{B}(t) - \omega_0/\gamma\hat{z} \\ &= B_1\hat{x}\prime + (B_0 - \omega_0/\gamma)\hat{z} \\ &= B_1\hat{x}.\end{aligned}$$

and therefore rotates with

$$\omega_R = \gamma B_1$$

Magnetic Resonance

off resonance

a)

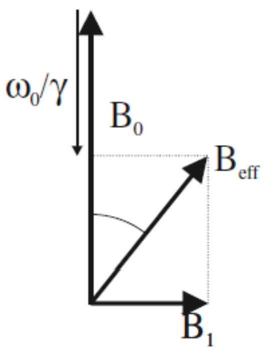

Effective field in the rotating coordinate system

b)

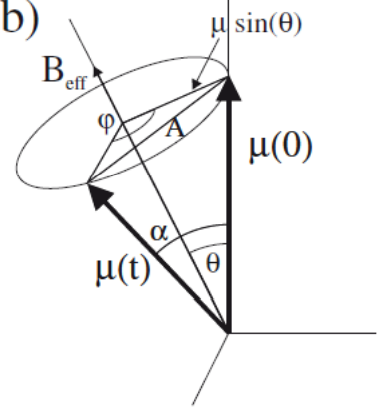

Motion of the magnetic moment in the effective magnetic field B_{eff}

c)

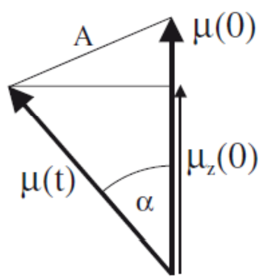

Projection of μ(t) on z-axis

effective magnetic field in rotating frame $\vec{B}_{eff} = B_1\hat{x}\prime + (B_0 - \omega/\gamma)\hat{z}$

effective Rabi frequency $\omega_{R\prime} = \gamma B_{eff} = \gamma\sqrt{(B_0 - \omega/\gamma)^2 + B_1^2} = \sqrt{(\omega_0 - \omega)^2 + \omega_R^2}$

Motion of magnetic moment $\mu_z(t) = \mu\left[1 - 2(\omega_R/\omega_R')^2\sin^2(\omega_R' t/2)\right]$

Spontaner Zerfall

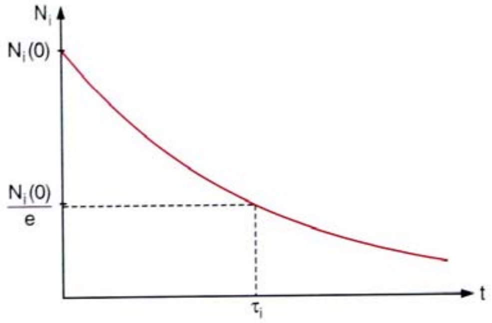

Abb. 7.13. Abklingkurve der Besetzungszahl $N_i(t)$ eines angeregten Zustandes bei zeitlich konstanter Zerfallswahrscheinlichkeit

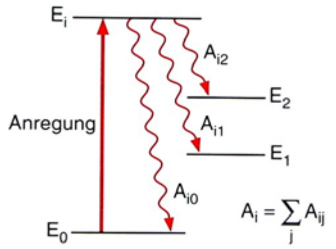

Abb. 7.12. Spontane Fluoreszenzübergänge vom angeregten Zustand E_i in tiefere Zustände E_j

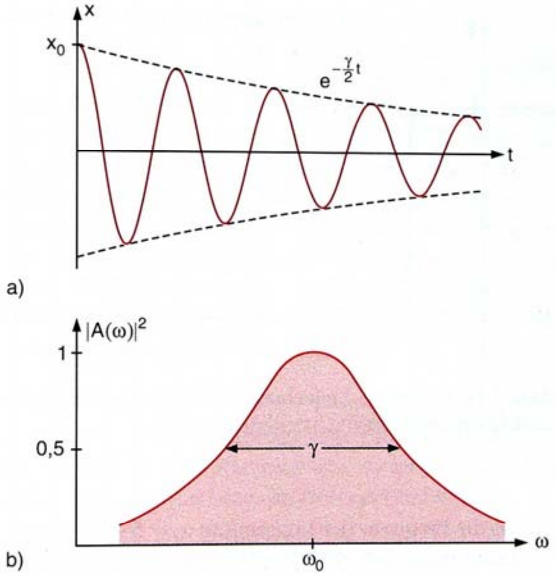

Abb. 7.17. (**a**) Gedämpfte Schwingung. (**b**) Linien-Lorentzprofil $|A(\omega)|^2$ als Fouriertransformierte einer gedämpften Schwingung

Spektrallinie

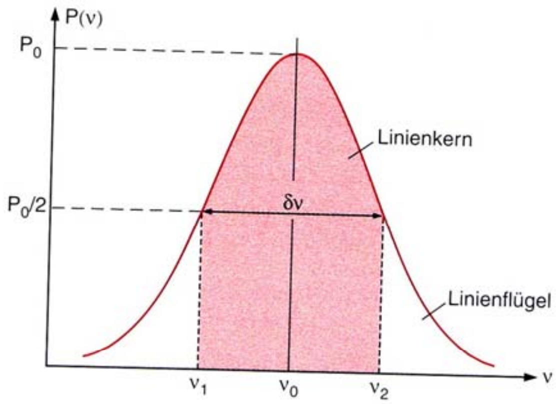

Abb. 7.16. Linienprofil einer Spektrallinie

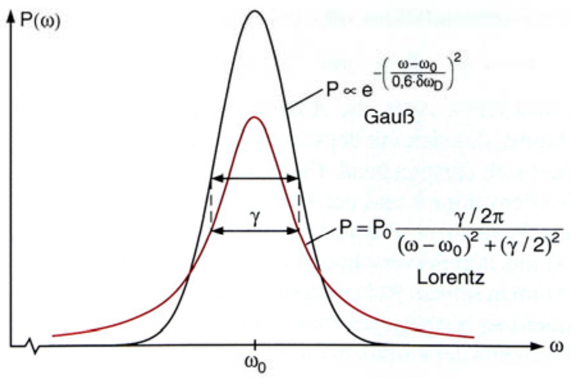

Abb. 7.20. Vergleich von Lorentzprofil und Gaußprofil mit gleicher Halbwertsbreite

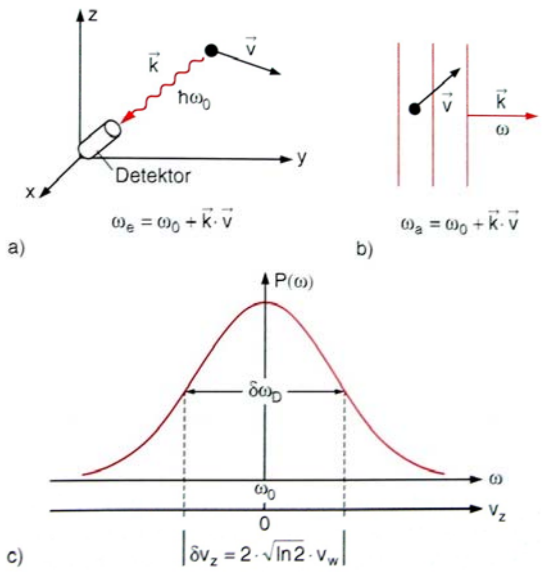

Zum Dopplereffekt

Verbreiterung der Linien
Stoßverbreiterung

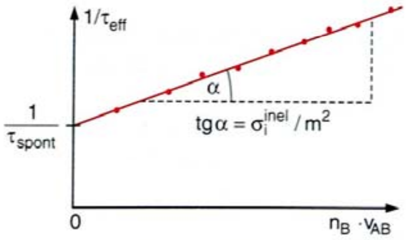

Abb. 7.15. Inverse effektive Lebensdauer $1/\tau_{eff}$ eines angeregten Zustandes als Funktion der Dichte der Stoßparameter *B* (Stern-Volmer-Plot)

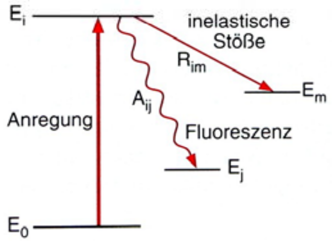

Abb. 7.14. Auch inelastische Stoßprozesse können zur Entvölkerung eines angeregten Zustandes beitragen

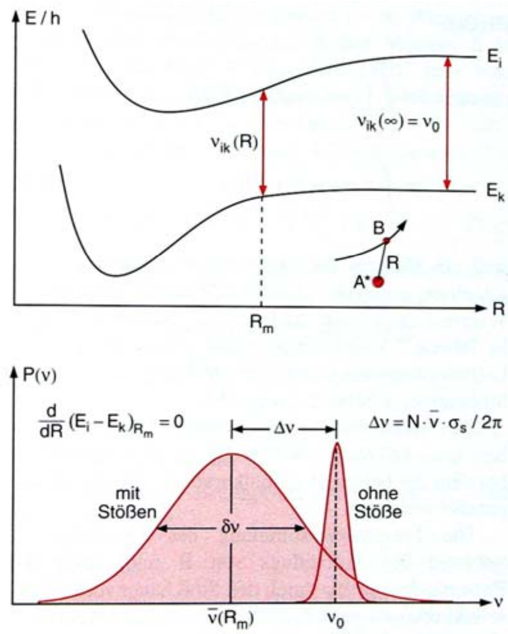

Abb. 7.21. Erklärung der Stoßverbreiterung und Verschiebung bei elastischen Stößen mit Hilfe der Potentialkurven des Stoßpaares

Rate Equations
regions of validity

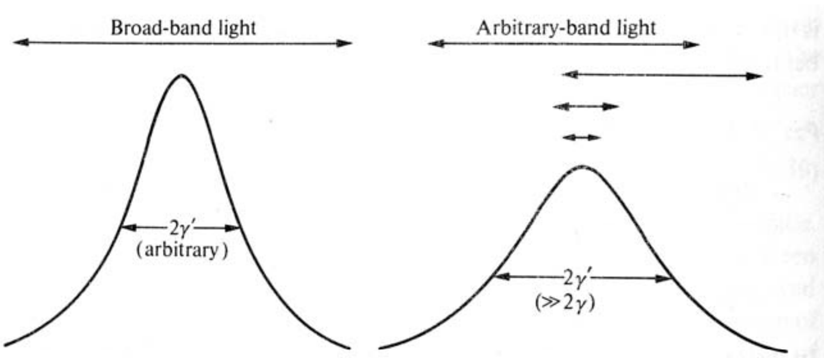

FIG. 2.13. Representations of the two regimes in which the optical Bloch equations reproduce the same atomic level populations as the Einstein-coefficient rate equations.

Monte Carlo Wave Function

J. Dalibard, Y. Castin, K. Moellmer: PRL **68** p580 (1992)

Problem: treatment of 'dissipative' processes in a wavefunction description
example: the coupling of atom + laser (small system) to the vacuum modes (reservoir)

standard approach: Master equation for the reduced density operator. in our case the optical Bloch equations
MCWF approach: simulate the dissipative events in 'gedanken experiments'.
The random detection event determines the wavefunction afterwards.

Simulating a quantum trajectory of the system: MCWF approach

wave function at time t: $|\psi(t)\rangle = |\phi(t)\rangle \otimes |0\rangle = (\alpha_g|g\rangle + \alpha_e|e\rangle) \otimes |0\rangle$

after a time step dt: $|\psi(t+dt)\rangle = |\psi^{(0)}(t+dt)\rangle + |\psi^{(1)}(t+dt)\rangle$,

no photon emitted $|\psi^{(0)}(t+dt)\rangle = (\alpha_g'|g\rangle + \alpha_e'|e\rangle) \otimes |0\rangle$,

1 photon emitted $|\psi^{(1)}(t+dt)\rangle = |g\rangle \otimes \sum_{\mathbf{k},\epsilon} \beta_{\mathbf{k},\epsilon} |\mathbf{k},\epsilon\rangle$.

probability of emitting a photon is dp

$$\langle \psi^{(0)} | \psi^{(0)} \rangle = 1 - \langle \psi^{(1)} | \psi^{(1)} \rangle = 1 - dp$$

after 'detection of the photon:

no photon detected $|\psi(t+dt)\rangle = \mu(\alpha_g'|g\rangle + \alpha_e'|e\rangle) \otimes |0\rangle$
$= \mu(1 - idtH)|\phi(t)\rangle \otimes |0\rangle$

renormalization of the WF due to 'no detection event' $\mu = (1-dp)^{-1/2}$

1 photon detected $|\psi(t+dt)\rangle = |g\rangle \otimes |0\rangle$

the full evolution is simulated by averaging over many single quantum trajectories

Example: damped Rabi oscillations:

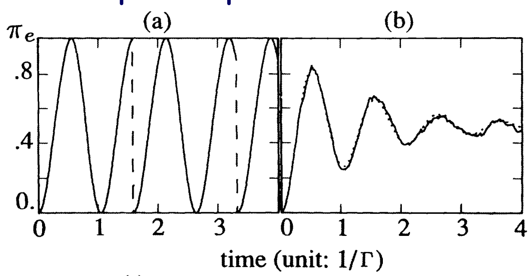

FIG. 1. (a) Time evolution of the excited-state population π_e of a two-level atom in the MCWF approach ($\Omega = 3\Gamma$, $\delta = 0$). The dashed lines indicate the projection of the atomic wave function onto the ground state after the detection of a spontaneous photon. (b) Average of $\pi_e(t)$ for 100 MCWF starting all in the ground state at $t=0$. The dotted line represents the result from the standard OBE treatment.

MCWF is an efficient tool:
for systems with N states, there are N equations for the wavefunction

OBE: N^2 equations to solve

Monte Carlo Wave Function

R. Dum, P. Zoller, H. Ritsch PRA **45**, 4879 (1992)

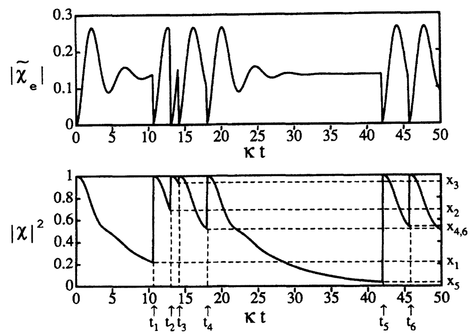

FIG. 1. Plot of a realization of the Monte Carlo wave function as a function of time: (a) excited-state probability $|\langle e|\tilde{\chi}(t)\rangle|^2$, (b) the corresponding norm $\| |\chi(t)\rangle \|^2$. The parameters are $\Omega = \kappa$ and $\Delta = -\kappa$.

more efficient simulation with quantum jumps

Integrate the non-Hermitian Schrödinger equation until the next decay step.

decay: $\frac{dC_2}{dt} = -i\gamma C_2$

driven two level system:

$$\Omega_{Rabi}\frac{1}{2}\exp(-i(\omega-\omega_0)t)C_2 = i\frac{dC_1}{dt}$$
$$\Omega^*_{Rabi}\frac{1}{2}\exp(i(\omega-\omega_0)t)C_1 - i\gamma C_2 = i\frac{dC_2}{dt}$$

In a MC formulation the emission of the photon is when the norm of the WF is below randomly defined value (MC simulation). With the 'photon detection' the WF is reset to a definite state, the detected state.

The quantum jump reduces the WF to the detected state

The full density matrix is simulated as the average of many MC trajectories.

$$\rho_A(t) \approx \frac{1}{N}\sum_{i=1}^{N} |\tilde{\chi}_i(t)\rangle\langle\tilde{\chi}_i(t)|$$

with $|\tilde{\chi}_i(t)\rangle = |\chi_i(t)\rangle / \| |\chi_i(t)\rangle \|$

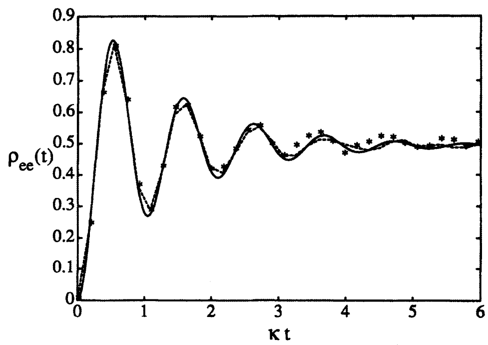

FIG. 2. Simulation predictions for the excited-state population $\rho_{ee}(t)$ are compared with the exact result derived from the optical Bloch equations. The stars correspond to 100 realizations. The dashed line has been computed with 1000 trajectories. For 10 000 realizations the simulation result is indistinguishable from the exact solution. The parameters are $\Omega = 6\kappa$ and $\Delta = 0$.